6 February 2002

Chemical Physics Letters 352 (2002) 499–504

CHEMICAL PHYSICS LETTERS

www.elsevier.com/locate/cplett

Dynamic force spectroscopy: a Fokker–Planck approach

O.K. Dudko [a,*], A.E. Filippov [b], J. Klafter [a], M. Urbakh [a]

[a] *Sackler Faculty of Exact Sciences, School of Chemistry, Tel Aviv University, Ramat Aviv, 69978 Tel Aviv, Israel*
[b] *Donetsk Institute for Physics and Engineering of NASU, 83144 Donetsk, Ukraine*

Received 17 October 2001

Abstract

In this Letter we show that recent observations using dynamic force spectroscopy can be described by a generalized Tomlinson model which includes the contribution of an external noise. We show that the measured friction forces depend on the microscopic potential and dissipation inherent to the system as well as on the mechanical properties of the setup (i.e. spring constant) and the external noise. Tuning the noise and spring constant offers ways to extract information about the microscopic properties. © 2002 Published by Elsevier Science B.V.

Experiments that probe mechanical forces on small scales provide a versatile tool for studying molecular adhesion and friction through the response to mechanical stress of single molecules or of nanoscale tips. The probing techniques include atomic force microscopy (AFM) [1,2], biomembrane force probe microscopy [3] and optical tweezers [4]. Examples for processes which are investigated are friction on atomic scale [1,2], specific binding of ligand–receptor [5], protein unfolding [6], and mechanical properties of single polymer molecules such as DNA [7]. In these experiments one probes forces along a reaction coordinate. Recent theoretical studies [8–10] suggest that microscopic information on the potential and dissipative interactions, which a molecule or a tip experiences, can be obtained from dynamic force spectroscopy (DFS) by investigating the velocity dependence of the mechanical forces.

Here we introduce a generalization of the Tomlinson model [11] to describe the dynamical response of a tip subject to a lateral drive in the context of DFS. The one-dimensional Tomlinson model has proven powerful in describing the response of a tip in AFM configurations and in reproducing many of the experimental observations [12,13]. Our generalization of the Tomlinson model is by including thermal fluctuations. Introducing thermal fluctuations leads to a Langevin equation of motion which describes the AFM response, namely the lateral motion of a driven tip,

$$M\ddot{x}(t) = -\eta\dot{x}(t) - \frac{\partial U(x)}{\partial x} - K(x - Vt) + \Gamma(t). \quad (1)$$

Here the driven tip is of mass M whose lateral coordinate x is pulled by a spring of a spring constant K. $U(x) = U_0\cos(2\pi x/b)$ is the periodic potential experienced by the tip due to the interactions with the substrate. This choice of a

* Corresponding author. Fax: +972-3-640-9293.
E-mail address: dudko@post.tau.ac.il (O.K. Dudko).

0009-2614/02/$ - see front matter © 2002 Published by Elsevier Science B.V.
PII: S0009-2614(01)01469-5

periodic potential allows for a quantitative analysis of the dynamics by reducing the number of parameters. Generalizations to non-periodic potential are possible. The parameter η is responsible for the dissipation which arises from interaction with phonons and/or other excitations. The spring is connected to a stage which is driven with a constant velocity V. In contrast to the previous studies of the Tomlinson model, Eq. (1) includes also the effect of noise given by a random force $\Gamma(t)$, which is δ-correlated $\langle\Gamma(t)\Gamma(0)\rangle = \Delta^2\delta(t)$. For thermal fluctuations $\Delta^2 = 2k_{\mathrm{B}}T\eta$.

It is convenient to introduce the dimensionless space and time coordinates, $y = 2\pi x/b$ and $\tau = t\omega$, where $\omega = (2\pi/b)(U_0/M)^{1/2}$ is the frequency of the small oscillations of the tip in the minima of the periodic potential. The dynamical behavior of the system is determined by the following dimensionless parameters: $\alpha = (\Omega/\omega)^2$ is the square of the ratio of the frequency of the free oscillations of the tip $\Omega = \sqrt{K/M}$ to ω. $\hat{\eta} = \eta/(M\omega)$, $\sigma^2 = \Delta^2/(U_0\eta)$, and $\hat{V} = 2\pi V/(\omega b)$ are, respectively, the dimensionless dissipation constant, intensity of the noise, and stage velocity. Eq. (1) describes also the response of macromolecules subject to an external drive provided for instance by optical tweezers.

The observable in DFS is the spring (or frictional) force, in particular its time series and dependencies on external parameters such as driving velocity, spring constant, temperature and normal load. The main result reported in DFS is $F(V)$, the velocity-dependent force, either maximal or time-averaged. In order to understand the nature of the force and to establish relationships between the measured forces and the microscopic parameters of the system we apply two approaches: (a) direct integration of the Langevin equation (1), and (b) reconstruction of the force from the density of states, which is accumulated from the corresponding Fokker–Planck equation [14]. In the Fokker–Planck approach the average friction force can be written as

$$F = \int_{x,v}\int \rho(x,v;V,\sigma)(\sin(2\pi x/b) + \eta v)\,\mathrm{d}x\,\mathrm{d}v, \qquad (2)$$

where v is a tip velocity in response to V and $\rho(x,v;V,\sigma)$ is a time-averaged density of states for the driven tip in phase space $\{x,v\}$. This equation explicitly demonstrates two contributions to the friction force: the potential given by the $\sin(2\pi x/b)$ term and the viscous one given by the ηv term.

Fig. 1 shows the velocity dependence of the time-averaged forces found through direct numerical solution of Eq. (1) and by using Eq. (2), namely the Fokker–Planck approach. The time-averaged forces in our periodic potential provide the same information as that of an ensemble of tips pulled over a barrier.

All calculations have been done under the condition $\alpha < \hat{\eta}^2/4 < 1$, when the system is underdamped with respect to the periodic potential and overdamped with respect to the driven spring. Under these conditions we find that for low driving velocities the system exhibits well-defined stick-slip motion with a positive minimal spring force, that is usually observed in AFM measurements [1,2].

The Langevin and Fokker–Planck approaches should be equivalent when exact calculations are possible, however as approximations they can provide complimentary information on the dynamics of the system. Here we concentrate on averaged forces, however more information can be obtained from detailed analysis of the time series which characterizes the response of the system [15,16].

At low temperatures the velocity dependence of the averaged force clearly exhibits the existence of two different regimes of motion: at low driving velocities $F(V)$ depends only slightly on V, while for higher velocities $F(V)$ approaches ηV. The first regime corresponds to stick-slip motion in the time series and the second one to sliding. Increasing the temperature leads to an irregular motion of the tip and smears out the difference between these regimes. It should be noted that for relatively strong spring constants K, when α is of the order of η^2, spikes are observed in the averaged force for a weak noise, see Fig. 1a. These spikes correspond to parametric resonances which arise under oscillating driving forces [17]. They are smoothed out for weaker springs and/or stronger fluctuations.

The thermal fluctuations contribute to the response of the tip in two opposite directions:

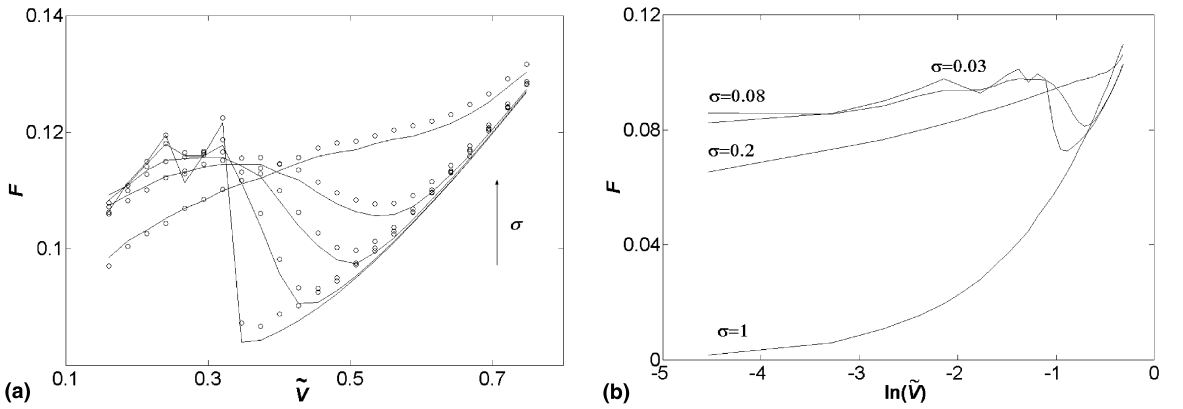

Fig. 1. An average frictional force as a function of driving velocity (a), and of the logarithm of the driving velocity (b) in dimensionless units. Solid lines and circles show the forces found by using Eqs. (1) and (2), respectively. The arrow indicates growing intensity of noise. Parameter values: $\sigma = 0$, 0.05, 0.08, 0.1, 0.2; $\alpha = 7 \times 10^{-3}$, $\tilde{\eta} = 0.2$.

(a) they help in getting out of locked states at the minima of the total potential

$$\Phi(X,t) = U_0 \cos_0\left(\frac{2\pi}{b}x\right) + \frac{K}{2}(x - Vt)^2,$$

and (b) they can make a sliding tip return back to a locked state. Therefore the fluctuation-assisted motion is expected to cause a decrease in the mean frictional force at low velocities, when the activation over the potential dominates. At high velocities the second effect becomes relevant and causes the observed enhancement of the friction in the sliding regime. These behaviors have been actually found in our simulations (see Fig. 1a).

Both effects of the fluctuations are clearly reflected in the projections of the time-averaged density of states $\rho(x, v; V, \sigma)$ on x and v, which are shown in Fig. 2. The density ρ has been accumulated over long periods of time, and in order to improve the averaging process we considered an ensemble of tips. In the stick-slip regime (low driving velocities V) $\rho(x, v; V, \sigma)$ exhibits two maxima as a function of v, a sharp one at $v = 0$, and a less pronounced one at $v \neq 0$ (see Fig. 2a). These maxima reflect the existence of two well-defined states, locked and sliding states. Increasing the intensity σ^2 of the noise leads to a decrease in the density of locked states at the cost of an increase of the sliding states. This is reflected in the temperature dependence of the friction force described above. In the sliding regime (high driving velocities) the density of states is localized around $v = V$, and the contribution of the locked state is small. Fig. 2b shows that the density as a function of the coordinate for the locked states is concentrated near the minimum of the potential, while for the sliding state it is approximately uniform along the space coordinate. Using Eq. (2) and the phase space properties of the density of states we conclude that locked states contribute mostly to the *potential* component of the friction force that

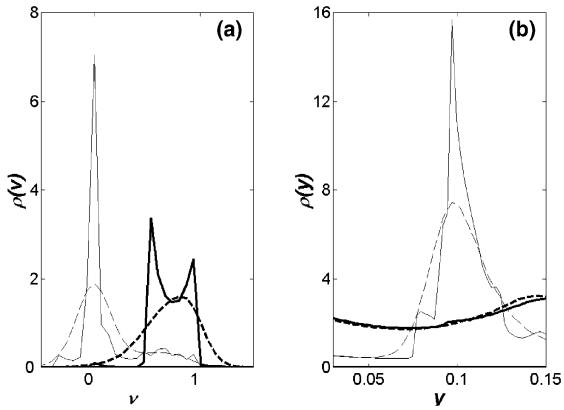

Fig. 2. Projections of the time-averaged density of states on the velocity (a) and coordinate (b) of the tip for the driving velocities $\tilde{V} = 0.15$ (thin lines) and $\tilde{V} = 0.7$ (bold lines) and noise amplitudes $\sigma = 0.03$ (solid lines) and $\sigma = 0.2$ (dashed lines). Parameter values as in Fig. 1.

dominates at low driving velocities, and sliding states contribute to *viscous* friction dominating at high driving velocities.

The force $F(V)$ measured in DFS is usually plotted versus $\ln V$ based on the theoretical assumption supported by experiments [2,9,10,18] that $F \propto k_B T \ln V$. In Fig. 1b we test this assumption of the logarithmic dependence of the averaged force on V. Our results clearly show that the logarithmic variation of $F(V)$ is certainly not universal. This behavior is valid here only over a limited range of the intensities σ^2. For weak and strong fluctuations the behavior of $F(V)$ deviates from the logarithmic one. For weak spring constants, $\alpha/\hat{\eta}^2 \ll 1$, the logarithmic behavior becomes more pronounced and holds over a wider range of parameters σ and V. The dependence of the averaged frictional forces on the driving velocity and noise intensity, as shown in Fig. 1, agrees with what is found experimentally: logarithmic dependence on the external velocity and the dependence on the potential [2]. The maximal friction force calculated for various values of σ^2 basically behaves the same way.

We suggest below a simple analytical model, which describes the influence of the fluctuations on the density of locked states. The locked states, as mentioned, determine the friction in the region of low driving velocities. In the absence of noise the driven tip leaves a locked state (a minimum of the total potential $\Phi(x,t)$) only when the potential barrier vanishes, i.e. at the instability point where $d^2\Phi/dx^2 = 0$. At this point the spring force reaches the maximum value of $2\pi U_0/b$. In the presence of noise the transition to sliding occurs earlier, and the probability $P_0(t)$ to find the tip in the locked state is given by the following kinetic equation:

$$\frac{dP_0(t)}{dt} = -\omega_0 P_0(t) \exp[-E(t)/k_B T], \tag{3}$$

where $E(t)$ is the energy distance between neighboring minimum and maximum of the potential $\Phi(x,t)$ and ω_0 is the characteristic frequency of the order of $(2\pi/b)(U_0/M)^{1/2}$. In a locked state the time dependence of the tip position is given by the equilibrium condition $d\Phi(x,t)/dx = 0$. Calculating $P_0(x)$ and using Eq. (2) lead to the averaged friction force. We will however focus on the maximal spring force, measured in DFS, which is also simpler to calculate.

The value of the activation energy $E(t)$ changes between $2U_0$, at zero driving force, and 0 at the instability point. For a weak spring, $\alpha^2 \ll 1$, near the instability point, $E(t)$ can be written in the form $(V > 0)$

$$E(t) = (2\pi U_0/b - KVt)^{3/2}/[(U_0)^{1/2}(\pi/b)^{3/2}]. \tag{4}$$

Solving Eq. (3) with $E(t)$ given by Eq. (4) we obtain

$$\begin{aligned} P_0(t) \approx \exp\Bigg\{ & \frac{\omega_0}{3KV}(k_B T)^{2/3}\left(\left(\frac{2\pi}{b}\right)^3 U_0\right)^{1/3} \\ & \times \Bigg[-\gamma\left(\frac{2}{3}, \frac{2\sqrt{2}U_0}{k_B T}\right) \\ & + \gamma\left(\frac{2}{3}, \frac{1}{k_B T}\left(\left(\frac{2\pi}{b}\right)^3 U_0\right)^{-1/2}\right) \\ & \times \left(\frac{2\pi}{b}U_0 - KVt\right)^{3/2}\Bigg]\Bigg\}, \end{aligned} \tag{5}$$

where $\gamma(\alpha, t)$ is the incomplete gamma-function [19]. Using Eq. (5) the maximal spring force can be written as

$$\begin{aligned} F_{\max} &= -\max\left\{\frac{\partial U(x(t))}{\partial x} P_0(t)\right\}_t \\ &= 2\pi U_0/b - \frac{1}{2}(k_B T)^{2/3}[U_0(2\pi/b)^3]^{1/3} \\ &\quad \times \left[\ln\left(V\frac{Kb}{2\pi U_0 \omega_0}\right)\right]^{2/3}. \end{aligned} \tag{6}$$

The dependence of F on V given by Eq. (6) is close to a logarithmic dependence for driving velocities $\tilde{V} > \alpha$. For $\tilde{V} < \alpha$ velocity dependence is $F(V) \sim (\ln V)^{2/3}$. This result differs from the previous phenomenological estimations of the maximal spring force that predicted only a logarithmic variation of $F(V)$. It should be noted that Eq. (6) includes explicitly the dependence of the force on the parameters of the microscopic underlying potential and the macroscopic spring constant K. This equation can be used also for the other types of underlying potentials, for instance for elastic

contacts, where logarithmic-type behaviors were also observed [20].

Additional information on the effect of fluctuations on the dynamics of friction can be obtained from the analysis of other observables. Studying a random process it is natural to consider the time evolution of the variance of the displacement, ΔL, of the driven tip. In order to calculate these quantities we consider an ensemble of tips initially placed at the same point on the substrate. Fig. 3 displays the time evolution of the size of the spatial 'spot', S, which is the span of the ensemble of driven tips. At short times ΔL and S have maxima when most of the tips slide, and minima when they are locked. These limiting values come together as the time increases showing that at any given moment the two types of motion mix. Typical stages of the time evolution of the spot are presented in Fig. 4 showing the density distribution in the phase space.

The time evolution of S demonstrates that after a few stick-slip periods the spot reaches its maximal size that equals to a length of sliding of the individual tip. The variance of the displacement shows however a long time redistribution of the density inside the spot. The bottom envelop of $\Delta L(t)$ follows the time dependence of the mean square displacement for the Ornstein–Uhlenbeck process that describes diffusion in a harmonic potential, supplied here by the spring, $\Delta L(t) = [k_B T(1 - \exp(-2Kt/\eta_{\text{eff}}))/K]^{1/2}$ [14]. This results from the fact that during sliding the tips diffuse in the combined potential $\Phi(x,t)$ which for a weak spring is harmonic with slight modulations due to the periodic potential of the substrate.

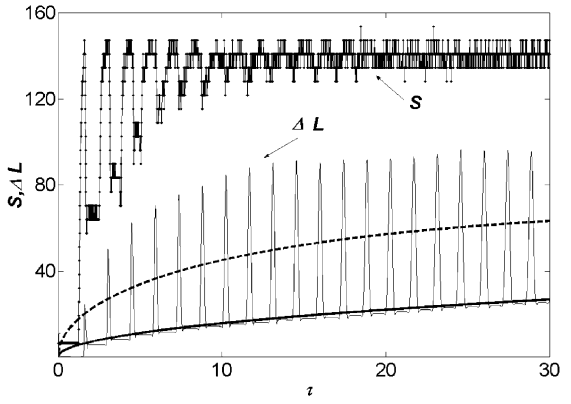

Fig. 3. Time evolution of the size S of the spatial 'spot' created by the ensemble of driven tips and of the variance of the displacement, ΔL. Solid and dashed lines show the envelops calculated according to the Ornstein–Uhlenbeck equation for the noise intensities $\sigma = 0.03$ and $\sigma = 0.3$. Parameter values: $\alpha = 3.2 \times 10^{-3}$, $\tilde{\eta} = 0.2$, $\tilde{V} = 0.45$.

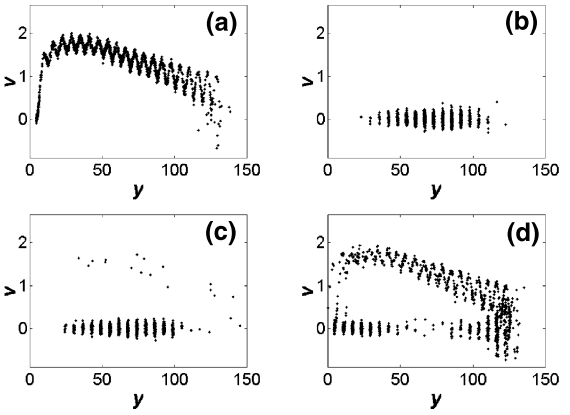

Fig. 4. Time evolution of the density of states distribution in the phase space. Typical stages of the time evolution of the portrait are presented: (a) the first jump of the tip from the locked state, (b) the locked state at short times, (c) intermediate stage of the time evolution, (d) stationary shape of the phase portrait showing mixing of locked and sliding states. All portraits are shown within the same interval of the space coordinates. Parameter values as in Fig. 3.

It should be noted that in order to fit the Ornstein–Uhlenbeck equation to the results of our calculations, the damping coefficient η_{eff} entered the equation should be considered as a fitting parameter that is inversely proportional to the intensity of the noise. This reflects the influence of the substrate potential that traps tips leading to an increase of the effective friction η_{eff}. This effect is most important at low intensities of the noise. Thus, envelopes of $\Delta L(t)$ and $S(t)$ become steeper as σ increases, and they approach asymptotic values at shorter times (see Fig. 3).

In conclusion, DFS results depend not only on the underlying potential and dissipative interaction but also on the intensity of external noise and on the driven spring constant. Tuning these parameters allows to separate the potential and dissipative contributions to the force and to extract desirable information on the microscopic properties of the

system. The amplitude of our periodic potential can be deduced from F_{max}. Increasing the intensity of the noise makes the dissipative component of friction ηV dominate already at low driving velocities and enable to obtain η experimentally.

Acknowledgements

Financial support for this work by grants from the Israel Science Foundation, BSF, TMR-SISITOMAS and DIP is gratefully acknowledged.

References

[1] R.M. Overney et al., Phys. Rev. Lett. 76 (1996) 1272.
[2] E. Gnecco et al., Phys. Rev. Lett. 84 (2000) 1172.
[3] R. Merkel et al., Nature (London) 397 (1999) 50.
[4] A.D. Mehta et al., Science 283 (1999) 1689.
[5] E.-L. Florin, V.T. Moy, H.E. Gaub, Science 264 (1994) 415.
[6] M. Rief et al., Science 276 (1997) 1109;
A.F. Oberhauser et al., Nature (London) 393 (1998) 181.
[7] G.U. Lee, L.A. Chrisey, R.J. Colton, Science 266 (1994) 771.
[8] J. Shillcock, U. Seifert, Phys. Rev. E 57 (1998) 7301.
[9] B. Heymann, H. Grubmüller, Phys. Rev. Lett. 84 (2000) 6126.
[10] E. Galligan et al., J. Chem. Phys. 114 (2001) 3208.
[11] G.A. Tomlinson, Philos. Mag. 7 (1929) 905.
[12] T. Gyalog, H. Thomas, Z. Phys. B 104 (1997) 669.
[13] V. Zaloj, M. Urbakh, J. Klafter, Phys. Rev. Lett. 82 (1999) 4823.
[14] H. Risken, The Fokker–Planck Equation, Springer, Berlin, 1996.
[15] M.G. Rozman, M. Urbakh, J. Klafter, Phys. Rev. Lett. 77 (1996) 683.
[16] M.G. Rozman, M. Urbakh, J. Klafter, F.-J. Elmer, J. Phys. Chem. 102 (1998) 7924.
[17] J.S. Helman, W. Baltensperger, J.A. Hoist, Phys. Rev. B 49 (1994) 3831.
[18] T. Bouhacina et al., Phys. Rev. B 56 (1997) 7694.
[19] I.S. Gradshtein, I.M. Ryzhik, Table of Integrals, Series, and Products, Academic Press, New York, 1980.
[20] F. Heslot et al., Phys. Rev. E 49 (1994) 4973.